

# Excitation-emission matrix (EEM) fluorescence spectroscopy for characterization of organic matter in membrane bioreactors: Principles, methods and applications

Jinlan Yu<sup>1</sup>, Kang Xiao (✉)<sup>1,2,3</sup>, Wenchao Xue<sup>4</sup>, Yue-xiao Shen<sup>5</sup>, Jihua Tan<sup>1</sup>, Shuai Liang<sup>6</sup>, Yanfen Wang<sup>1,2</sup>, Xia Huang<sup>3,7</sup>

<sup>1</sup> College of Resources and Environment, University of Chinese Academy of Sciences, Beijing 100049, China

<sup>2</sup> CAS Center for Excellence in Tibetan Plateau Earth Sciences, Beijing 100101, China

<sup>3</sup> State Key Joint Laboratory of Environment Simulation and Pollution Control, School of Environment, Tsinghua University, Beijing 100084, China

<sup>4</sup> School of Environment, Resources and Development, Asian Institute of Technology, Klong Luang, Pathumthani 12120, Thailand

<sup>5</sup> Department of Civil, Environmental, and Construction Engineering, Texas Tech University, Lubbock, TX 79409, USA

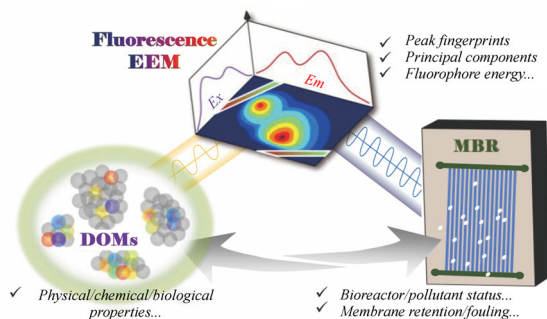
<sup>6</sup> College of Environmental Science and Engineering, Beijing Forestry University, Beijing 100083, China

<sup>7</sup> Research and Application Center for Membrane Technology, School of Environment, Tsinghua University, Beijing 100084, China

## HIGHLIGHTS

- Principles and methods for fluorescence EEM are systematically outlined.
- Fluorophore peak/region/component and energy information can be extracted from EEM.
- EEM can fingerprint the physical/chemical/biological properties of DOM in MBRs.
- EEM is useful for tracking pollutant transformation and membrane retention/fouling.
- Improvements are still needed to overcome limitations for further studies.

## GRAPHIC ABSTRACT



## ARTICLE INFO

### Article history:

Received 10 October 2019

Revised 7 November 2019

Accepted 28 November 2019

Available online 15 January 2020

### Keywords:

excitation-emission matrix (EEM)  
dissolved organic matter (DOM)  
membrane bioreactor (MBR)  
fluorescence indicator  
characterization method

## ABSTRACT

The membrane bioreactor (MBR) technology is a rising star for wastewater treatment. The pollutant elimination and membrane fouling performances of MBRs are essentially related to the dissolved organic matter (DOM) in the system. Three-dimensional excitation-emission matrix (3D-EEM) fluorescence spectroscopy, a powerful tool for the rapid and sensitive characterization of DOM, has been extensively applied in MBR studies; however, only a limited portion of the EEM fingerprinting information was utilized. This paper revisits the principles and methods of fluorescence EEM, and reviews the recent progress in applying EEM to characterize DOM in MBR studies. We systematically introduced the information extracted from EEM by considering the fluorescence peak location/intensity, wavelength regional distribution, and spectral deconvolution (giving fluorescent component loadings/scores), and discussed how to use the information to interpret the chemical compositions, physiochemical properties, biological activities, membrane retention/fouling behaviors, and migration/transformation fates of DOM in MBR systems. In addition to conventional EEM indicators, novel fluorescent parameters are summarized for potential use, including quantum yield, Stokes shift, excited energy state, and fluorescence lifetime. The current limitations of EEM-based DOM characterization are also discussed, with possible measures proposed to improve applications in MBR monitoring.

© Higher Education Press and Springer-Verlag GmbH Germany, part of Springer Nature 2020

## 1 Introduction

Membrane bioreactors (MBRs) are widely applied in

wastewater treatment and reclamation and have been proved to be an effective and promising technology. Compared with the conventional activated sludge process with secondary sedimentation, MBR has numerous advantages including small footprint, high effluent quality, complete separation of sludge retention time (SRT) from

✉ Corresponding author  
E-mail: kxiao@ucas.ac.cn

hydraulic retention time (HRT), and enhanced pollutant degradation (Xia et al., 2015; Xiao et al., 2019b). Research on MBR has mainly included the following aspects: (a) the pollutant removal efficiency (Echevarría et al., 2019), (b) process and module configurations (Yan et al., 2015), (c) operational conditions (Menniti and Morgenroth, 2010), (d) operating cost and energy consumption (Echevarría et al., 2019; Xiao et al., 2019b), (e) the behavior of pollutants and microorganisms in the system (Jacquin et al., 2018a; Tan et al., 2019), and (f) the mechanism and control of membrane fouling (Lin et al., 2013; Xiao et al., 2014).

Dissolved organic matter (DOM), a highly heterogeneous mixture (e.g., microbial byproducts and undegraded residues) in the MBR system, has a profound influence on the biochemical processes of pollutants (Hudson et al., 2008), stability and transfer of particulate matter (Xiao et al., 2018c), complexation of metals (Chen et al., 2013), formation of disinfection byproducts (DBPs) (Ma et al., 2018), and development of membrane fouling (Wang et al., 2009; Tang et al., 2010). Therefore, it is essential to monitor DOM characteristics for effective and stable operation of an MBR. Several methods have been applied to determine the organic matter concentration. For example, the total organic carbon (TOC) reflects the overall amount of organic matter; the DuBois (DuBois et al., 1956) and Lowry methods (Lowry et al., 1951) quantify the polysaccharide, protein, and humic contents; DAX (or XAD) resin column chromatography fractionates the hydrophobic/hydrophilic components (Mu et al., 2019); size-exclusion chromatography–organic carbon detection–organic nitrogen detection (LC-OCD-OND) characterizes the molecular weight distribution in terms of organic carbon and nitrogen (Huber et al., 2011; Jacquin et al., 2017); and a more advanced technique, Fourier transform ion cyclotron resonance mass spectrometry (FT-ICR-MS), elaborates the mass composition at the molecular level (Ly and Hur, 2018). UV–visible absorption spectroscopy is also widely used to quantify components in water (Figueiró et al., 2018). However, the above methods (except UV–visible spectroscopy) are usually laborious and time-consuming, and inefficient for rapid monitoring of DOM. Conversely, three-dimensional excitation–emission matrix (3D-EEM) is a convenient, highly sensitive, and selective method that does not destroy samples. An EEM contains a vast amount of fingerprinting information for DOM, including the chemical composition (Coble, 1996), hydrophobicity (Xiao et al., 2018b), molecular weight (Cuss and Guéguen, 2015), humification degree (Huguet et al., 2009), microbial activity (Dong et al., 2010), and DBP formation potential (Ma et al., 2018). Furthermore, EEM has great potential in achieving online monitoring of DOM. Due to these advantages, EEM has attracted attention in the area of MBR research and resulted in an increasing number of applications for the characterization, indication, and

elucidation of DOM behavior, pollutant transformation, biomass properties, and membrane performance over the past decade (Wang et al., 2009; Liu et al., 2011; Zhuo et al., 2018). Nevertheless, the EEM-derived information that has been utilized in MBR research is just the tip of the iceberg. The known EEM indicators need to be systematically summarized, and the to-be-exploited EEM information merits critical discussion for the sake of future studies.

This review aims to comprehensively summarize the principles of fluorescence, experimental methods of EEM, mathematical/statistical handling of data, information obtained from the spectra, and the relations of EEM indicators to DOM properties. We systematically outlined the applications of EEM in characterizing and controlling MBR processes and membrane fouling. Finally, the limitations of EEM and how to extend the applications of EEM in MBR are critically discussed.

---

## 2 EEM principles and measurements

### 2.1 Basic principles of fluorescence

When substances with fluorophores absorb light, the electrons that obtain energy undergo a transition and, after energy transfer, the electrons release energy back to the ground state, emitting light in the form of fluorescence. The mechanism of luminescence is shown in Fig. 1 (a Jablonski diagram), where  $S_0$ ,  $S_1$ ,  $S_2$ , and  $T_1$  represent different energy states of the electrons:  $S_0$  for the singlet ground state,  $S_1$  and  $S_2$  for the singlet excited states, and  $T_1$  for the triplet excited state. Each of these energy states includes several vibrational energy levels as depicted by 0, 1, 2, etc. Vibrational energy is prone to rapid dissipation, and the lowering of the energy level (in the same electronic state) is referred to as vibrational relaxation. Internal conversion is the rapid transition from a higher excited state to a lower excited state of the same spin multiplicity (e.g., from  $S_2$  to  $S_1$ ) whereas intersystem crossing is usually a much slower process of transition between two electronic states with different spin multiplicities (e.g., from  $S_1$  to  $T_1$ ). Fluorescence is emitted when  $S_1$  returns to  $S_0$  whereas phosphorescence is emitted when  $T_1$  returns to  $S_0$ . In the process of fluorescence, energy loss occurs due to internal conversion and vibrational relaxation, which results in a longer emission wavelength than the excitation wavelength (Lakowicz, 2006). The difference in the excitation and emission wavenumbers is called the Stokes shift. Note that fewer photons are normally emitted in the form of fluorescence than the photons absorbed for excitation of the electrons due to deactivation processes such as non-radiative decay of the excited electrons or quenching of the fluorescence. Quantum yield is defined as the ratio of the number of emitted photons to the number of absorbed photons and it is equal to the ratio of the measured lifetime to the intrinsic lifetime of the fluorophore (Wünsch et al., 2015).

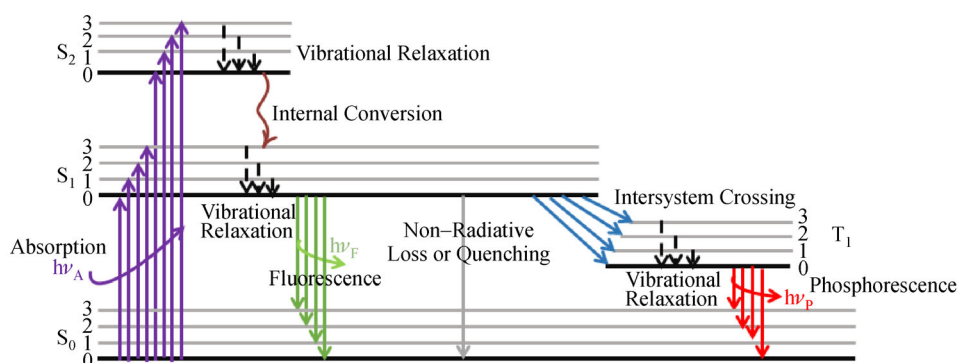


**Fig. 1** Schematic diagram of luminescence mechanisms.

Fluorescent molecules (fluorophores) generally possess  $\pi$ -conjugated systems and rigid planar structures. The degree of conjugation and rigidity, and the type of substituents in the molecule, affect the fluorescent properties (Lakowicz, 2006; Valeur and Berberan-Santos, 2012). The substituents include N, O, and S functional groups such as carboxyl, phenol, enol, hydroxyl, carbonyl, acyl, and thiols. These functional groups bound with unsaturated  $\pi$ -conjugated structures constitute a variety of fluorescent chemical compounds such as protein-like, humic-like, and fulvic-like substances (Leenheer and Croué, 2003; Wang et al., 2009). Therefore, DOM bearing these molecular segments can be monitored by fluorescence tools.

## 2.2 Fluorescence spectra types

Several fluorescence spectra have been applied in DOM characterization in ecosystems, including excitation spectra, emission spectra, synchronous fluorescence spectra, time-resolved fluorescence spectra, and EEM (Baker, 2001; Clark et al., 2002; Reynolds, 2003). EEM is measured by scanning the fluorescence intensity across a range of excitation (Ex) and emission (Em) wavelengths to generate an intensity–excitation–emission 3D graph. Compared with other fluorescence spectra, EEM results in a more comprehensive multidimensional detection of the fluorescence. The scanning is quick enough to allow for potential real-time online monitoring in water ecosystems and water treatment plants (Baker, 2001, 2002).

## 2.3 Methods for EEM measurement and data processing

EEM is measured using a fluorescence spectrophotometer that scans the fluorescence intensity at various excitation and emission wavelengths, generating a set of intensity–Ex–Em data. The operational Ex and Em for data logging are usually  $\geq 200$  nm and  $\geq 250$  nm, respectively. Some researchers recommended that the fluorescence intensity be recorded at  $Ex \geq 220$  nm due to the larger deviation in the measurement at lower Ex (Goletz et al., 2011). Prior to

EEM measurement, the DOM solution must be filtered to remove large particles (e.g., larger than 0.45  $\mu$ m). As an important factor that affects fluorescence (Murphy et al., 2014), the pH of the solution should be adjusted (and/or buffered) when it is necessary to exclude its impact for the purpose of the study. Compared with the pH, the ionic strength of the solution is usually considered to be less influential in fluorescence measurement (Murphy et al., 2014; Li et al., 2016).

As shown in Fig. 2, the steps for processing the original EEM data to obtain a standardized EEM spectrum are as follows: (a) reducing the Rayleigh and Raman scatterings by subtracting pure water background, and smoothing the remained scatterings using a cubic spline interpolation technique (Bahram et al., 2006); (b) correcting the inner-filter effect using UV–visible absorbances (UVA) at the same optical path length (the correction is considered valid when the maximum UVA in a 1 cm cell is less than 1.5) (Mobed et al., 1996; Kothawala et al., 2013); and (c) dividing the EEM data by the integral area of the Raman peak of pure water at  $Ex = 350$  nm to remove instrument-dependent intensity factors (Lawaetz and Stedmon, 2009). A large amount of fluorescence information can be extracted from EEM data, including the peak intensity, peak location and distribution, information discovered from spectral decomposition, and information related to electron/photon energy in the fluorescence process. The fluorescence information can include indicators for a variety of DOM properties and behaviors in natural aquatic systems, wastewater treatment plants, and MBRs.

## 3 DOM information obtained from EEM

### 3.1 Information based on peak location

#### 3.1.1 EEM regions indicating chemical composition

The fluorescence properties of different materials are different, resulting in different distributions of fluorescent

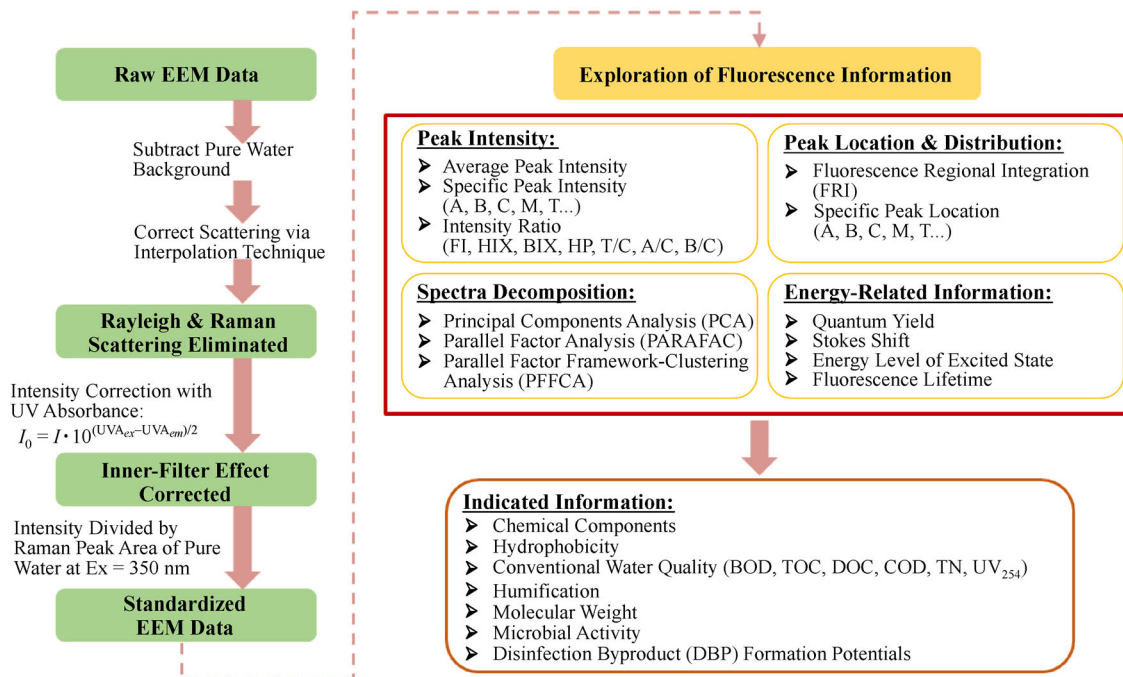


Fig. 2 Flow chart for EEM data processing.

peaks in the EEM spectra. The main fluorescent peaks of fluorescent dissolved organic matter (FDOM) are generally divided into five categories according to the chemical composition (Coble, 1996; Parlanti et al., 2000). As shown in Fig. 3(a), peak A,  $\alpha'$  [Ex/Em = (237–260)/(400–500) nm] and peak C,  $\alpha$  [Ex/Em = (300–370)/(400–500) nm] represent humic-like substances; peak M,  $\beta$  [Ex/Em = 312/(380–420) nm] represents marine humic-like substances; peak B,  $\gamma$  [Ex/Em = (270–280)/(300–320) nm] represents tyrosine-like protein substances; and peak T,  $\delta$  [Ex/Em = (270–280)/(320–350) nm] represents tryptophan-like protein substances. In addition, researchers proposed two other fluorescence peaks, peak D (Ex/Em = 390/509 nm) representing soil fulvic acid and peak N (Ex/Em = 280/370 nm) representing plankton-derived DOM (Stedmon et al., 2003).

The distribution of fluorescence in different Ex/Em wavelength regions of EEM is commonly related to the chemical composition of the DOM. Fluorescence region integration (FRI) provides an approach to characterizing the fluorescence distribution in different EEM spectral regions, and integrates the fluorescence intensity of each region to calculate the regional contribution to the total fluorescence (He et al., 2011; Jia et al., 2014; Xiao et al., 2018a). FRI divides an EEM spectrum into five main regions (Chen et al., 2003), as illustrated in Fig. 3(a). Regions I and II (Ex < 250 nm, Em < 380 nm) correspond to simple aromatic proteins such as tyrosine-like and tryptophan-like substances; region III (Ex < 250 nm, Em > 380 nm) corresponds to fulvic-like substances; region IV (Ex > 250 nm, Em < 380 nm) is related to soluble

microbial byproduct-like substances; and region V (Ex > 250 nm, Em > 380 nm) represents humic-like substances. Fluorescence peak identification and FRI analysis of EEM spectra have been widely used in MBR studies to track the transformation of DOM and investigate the major contributors to membrane fouling (Liu et al., 2011; Ma et al., 2014).

### 3.1.2 EEM regions indicating hydrophobicity and molecular weight

Hydrophobicity and molecular weight (MW) are basic properties of DOM. Hydrophobicity affects the interaction between DOM molecules and with other coexisting substances in the sludge mixture, thus affecting the migration and transformation behaviors of DOM in the environment and engineering systems (Wang and Chen, 2018). Previous research indicated that changes in DOM hydrophobicity during biological treatment and disinfection caused variations in biodegradability and biotoxicity of DOM (Liu et al., 2016). DOM can be divided into hydrophobic acids (HOA), hydrophobic bases (HOB), hydrophobic neutrals (HON), and hydrophilic substances (HIS) by DAX (or XAD) resin adsorption (Leenheer and Croué, 2003). HIS can be further subgrouped into hydrophilic acids/bases/neutrals (HIA/HIB/HIN) using ion-exchange resins (Leenheer and Croué, 2003). However, the resin fractionation method is complicated and time-consuming, making it difficult to achieve online monitoring of the hydrophobic/philic composition of DOM. EEM provides a convenient alternative in this

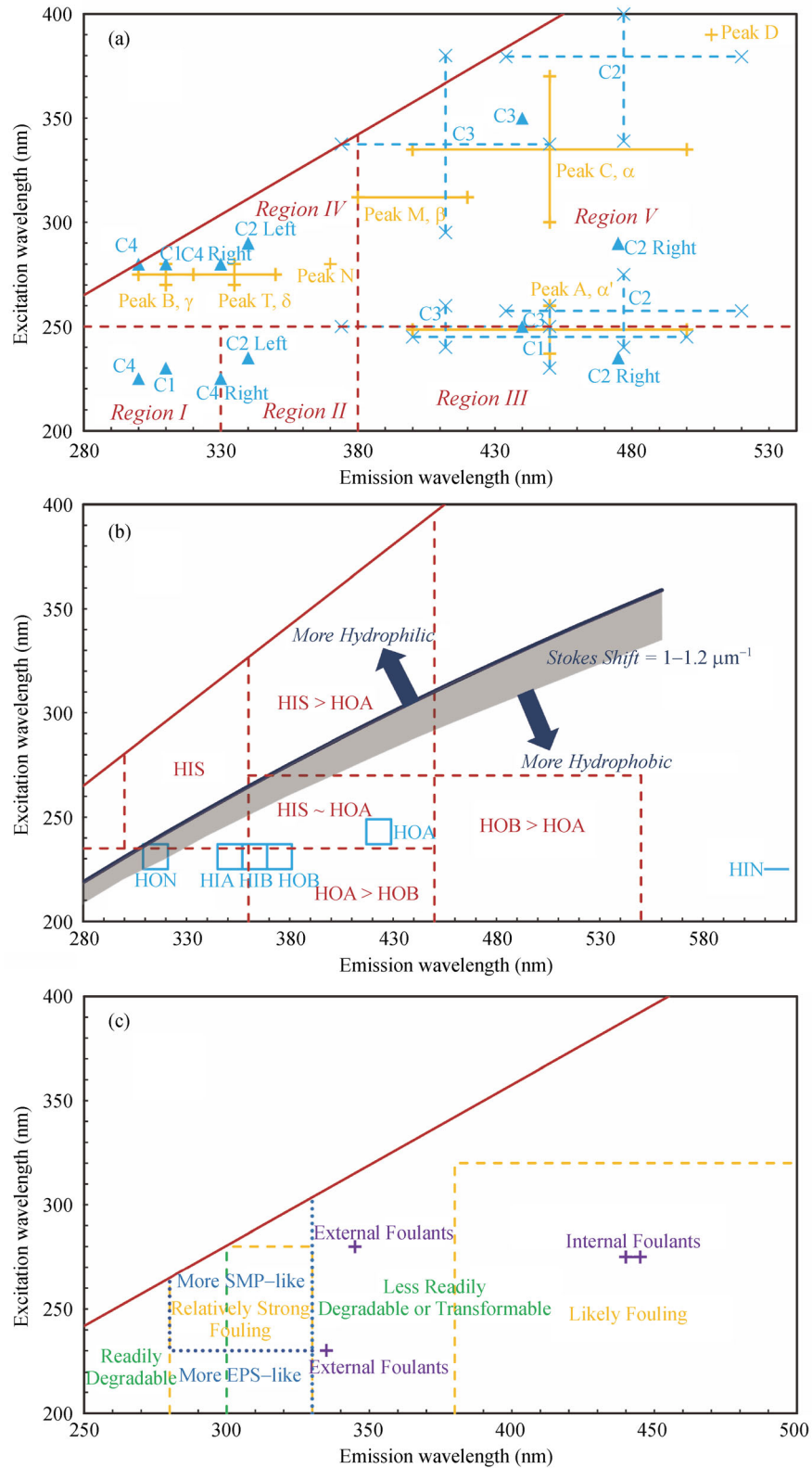


**Fig. 3** Collective depictions of fluorescence peaks and wavelength regions according to (a) chemical composition (Coble, 1996; Chen et al., 2003; Ishii and Boyer, 2012; Guo et al., 2018), (b) hydrophobicity (Marhaba et al., 2000; Xiao et al., 2016; Xiao et al., 2018b), and (c) functional behavior (Liu et al., 2011; Xiao et al., 2018a) of DOM in MBRs.

regard. Marhaba et al. (2000) applied EEM to efficiently characterize DOM in a wastewater treatment plant, demonstrating that different hydrophilic/hydrophobic components possessed different peak locations: HIA [Ex/Em = (225–237)/(345–357) nm], HIB [Ex/Em = (225–237)/(357–369) nm], HIN [Ex/Em = 225/(609–621) nm], HOA [Ex/Em = (237–249)/(417–429) nm], HOB [Ex/Em = (225–237)/(369–381) nm], and HON [Ex/Em = (225–237)/(309–321) nm]. Xiao et al. (2018b) found that the short wavelength region (Ex < 235 nm or Em < 300 nm) represented more HOA and HOB, and HIS tended to occur in the region where the Em was close to the Ex. The proportion of fluorescence in the Ex/Em = (200–400)/(300–550) nm region correlated significantly with the proportion of HIS in the overall TOC, and the significant correlation region for HOA was Ex/Em = (200–285)/(340–465) nm; HOB also exhibited a significant correlation but in a narrow region. Furthermore, hydrophobic components exhibited a greater quantum yield and Stokes shift than hydrophilic components, which is due to the higher aromaticity and larger scale of the  $\pi$ -conjugated system of hydrophobic components (Xiao et al., 2016; Xiao et al., 2019a). Therefore, EEM has the potential to indicate the hydrophobic/hydrophilic properties of DOM at qualitative or quantitative levels. A rough division of the fluorescence regions based on hydrophobicity is shown in Fig. 3(b).

The MW of DOM has also been related to the distribution of fluorescence on the EEM map. In MBR systems, the lower MW fractions were more prone to exhibit fluorescence in the lower wavelength range (Xiao et al., 2016; Xiao et al., 2018c), reflecting higher excited energy of the fluorescent groups in the lower MW molecules. However, unlike that for hydrophobicity, typical wavelength regions for different MW fractions have not yet been located on the EEM map.

### 3.1.3 EEM regions indicating DOM behaviors

The EEM map can also be divided into different fluorescence regions based on the behavior of the organic matter, including the biodegradability, sludge/water phase distribution (e.g., related to the balance between soluble microbial products (SMP) in the solution and extracellular polymeric substances (EPS) loosely/tightly bound to cells), and membrane fouling propensity. As shown in Fig. 3(c), Em = 300 nm can roughly divide the EEM spectrum into readily and less readily biodegradable regions (Xiao et al., 2018a); within the range of Em = 280–330 nm, the Ex > 230 nm region is more characteristic of SMP-like substances whereas Ex < 230 nm is more EPS-like (Xiao et al., 2018a); fluorescence prominent in the region of Em = 280–330 nm and Ex < 280 nm is a suspected trace of strong fouling propensity while that in the Ex = 200–350 nm and Em = 400–500 nm region is related to moderate fouling (Xiao et al., 2018a). Furthermore, a few fluores-

cence peaks in the Ex = 275 nm and Em = 440–445 nm region have been related to foulants causing internal fouling (inside the membrane pores) whereas Ex/Em = 230/350 nm and Ex/Em = 280/345 nm corresponded to external fouling (occurring in the form of a foulant layer on the membrane surface) (Liu et al., 2011).

## 3.2 Information based on peak intensity and intensity ratio

### 3.2.1 Indicators of water quality based on peak intensity

Fluorescence peak intensities are related to several water quality parameters, including biochemical oxygen demand (BOD), total organic carbon (TOC), dissolved organic carbon (DOC), chemical oxygen demand (COD), total nitrogen (TN), and UVA<sub>254</sub>. Numerous studies have investigated the correlations between fluorescence peak intensities and these parameters in water ecosystems and water treatment plants. As shown in Table 1, the TOC correlates well with protein-like and humic-like peak intensities (whereas Cumberland and Baker (2007) reported the lowest correlation coefficient, 0.167). Some studies reported a good correlation between the DOC and fluorescence peak intensities with correlation coefficients above 0.9 (Baghoth et al., 2011; Ignatev and Tuhkanen, 2019), but others reported low correlation coefficients such as 0.28 (Cumberland and Baker, 2007). The remarkable differences in correlation coefficients may result from the sources of DOM. The correlation coefficients between the BOD and protein-like peak intensity (or component score) ranged from 0.82 to 0.98 and those between the BOD and humic-like peak intensity (or component score) ranged from 0.70 to 0.95. Overall, the BOD was better related to protein-like peaks or protein-like components. In addition, the COD, TN, and UVA<sub>254</sub> also exhibited significant correlations with fluorescence peaks and fluorescence components. Together, although these correlations were obtained mostly in water ecosystems and conventional wastewater treatment plants, it is manifest that the fluorescence peak intensities and fluorescence component scores have great potential to be applied in online monitoring of water quality parameters in MBR systems.

### 3.2.2 Indicators of physical/chemical/biological characteristics based on peak intensity

Molecular weight (MW) shows a correlation with fluorescence peak intensity. For DOM from natural waters, Cuss and Guéguen (2015) reported that the MW was negatively correlated with the intensities of peak B and peak T (defined in Fig. 3(a)) ( $p < 0.001$ ), and positively correlated with the sum of the intensities of peaks A and C ( $p < 0.001$ ). For DOM in MBR systems, researchers found that smaller DOM molecules tended to have higher FI per TOC, probably due to the higher fluorophore density and the larger specific area for light exposure (Xiao et al., 2016;

**Table 1** Correlation between water quality parameters and fluorescence parameters (fluorescence peaks and components)

Water quality parameters	Water systems	Fluorescence peaks and correlation coefficients	References
TOC	Surface waters, sewage treatment plants and samples of pollution incidents	Tryptophan-like T1 (0.88); tryptophan-like T2 (0.80); humic-like A (0.87); humic-like C (0.81)	Hudson et al. (2008)
	Surface water, groundwater, sewage treatment plants	Fulvic-like C2 (0.17-0.76)	Cumberland and Baker (2007)
	Sewage treatment plant	Tryptophan-like T (0.989)	Christian et al. (2017)
DOC	Surface water, groundwater, sewage treatment plants	Humic-like C1 (0.28-0.63)	Cumberland and Baker (2007)
	Sewage treatment plants (conventional activated sludge treatment)	Total tryptophan-like (0.96); total tyrosine-like (0.98)	Ignatev and Tuhkanen (2019)
	Drinking water treatment plants	Humic-like C1 (0.96); humic-like C2 (0.97); humic-like C3 (0.94); protein-like C4 (0.94); humic-like C5 (0.95); humic-like C6 (0.93); protein-like C7 (0.91)	Baghoth et al. (2011)
	Sewage treatment plants	Protein-like C1 (0.85-0.99); humic-like C2 (0.99); humic-like C3 (0.79-0.98); humic-like C4 (0.99)	Cohen et al. (2014)
COD	Sewage treatment plants (conventional activated sludge treatment)	Total tryptophan-like (0.90); total tyrosine-like (0.94)	Ignatev and Tuhkanen (2019)
	Surface water (Gap River watershed; Korea)	Humic-like C1(0.98); humic-like C2 (0.97); tryptophan-like C3 (0.98)	Hur and Cho (2012)
	Sewage treatment plants	Tryptophan-like T1 (0.85)	Bridgeman et al. (2013)
	Surface water (Tyne catchment in North-East England)	Tryptophan-like T ( 0.65)	Baker and Inverarity (2004)
	Sewage treatment plants	Protein-like C1 (0.82-0.99); humic-like C2 (0.91); humic-like C3 (0.96); humic-like C4 (0.80)	Cohen et al. (2014)
BOD	Surface waters, sewage treatment works and samples of pollution incidents	Tryptophan-like T1 (0.91); tryptophan-like T2 (0.85); humic-like A (0.70); humic-like C (0.77)	Hudson et al. (2008)
	Sewage treatment plants (conventional activated sludge treatment)	Total tryptophan-like (0.93); total tyrosine-like (0.96)	Ignatev and Tuhkanen (2019)
	Surface water (Gap River watershed; Korea)	Humic-like C1 (0.95); humic-like C2 (0.94); tryptophan-like C3 (0.95)	Hur and Cho (2012)
	Sewage treatment plants	Tryptophan-like T1 (0.89-0.94)	Reynolds and Ahmad (1997)
	Sewage treatment plants	Tryptophan-like T (0.97)	Ahmad and Reynolds (1999)
	Sewage treatment plants	Tryptophan-like T1 (0.92)	Bridgeman et al. (2013)
	Surface water (Tyne catchment in North-East England)	Tryptophan-like T (0.85)	Baker and Inverarity (2004)
	Landfill sites (North England)	Tryptophan-like T2 (0.94-0.98)	Baker and Curry (2004)
	Sewage treatment plants	Protein-like C1 (0.82) humic-like C2 (0.72)	Cohen et al. (2014)
	Sewage treatment plant	Tryptophan-like T (0.971); peak C (0.945)	Christian et al. (2017)
	TN	Surface water (Gap River watershed; Korea)	Humic-like C1 (0.951); humic-like C2 (0.927); tryptophan-like C3 (0.950)
Sewage treatment plants		Protein-like C1 (0.86-0.90); humic-like C2 (0.88); humic-like C3 (0.80); humic-like C4 (0.83)	Cohen et al. (2014)
UVA <sub>254</sub>	Drinking water treatment plants	Humic-like C1 (0.89); humic-like C2 (0.91); humic-like C3 (0.88); protein-like C4 (0.92); humic-like C5 (0.89); humic-like C6 (0.91); protein-like C7 (0.86)	Baghoth et al. (2011)
	Sewage treatment plants	Protein-like C1 (0.80-0.92); humic-like C2 (0.75-0.85); humic-like C3 (0.70-0.84); humic-like C4 (0.76)	Cohen et al. (2014)

Xiao et al., 2018c; Xiao et al., 2019a). In addition, it was reported that  $\log(\text{MW})$  (MW ranging from 1 kDa to 0.7  $\mu\text{m}$ ) was negatively correlated with the relative intensity, FI/TOC or FI/UVA, which was particularly significant in the shorter wavelength range of  $\text{Ex} < 300 \text{ nm}$  and  $\text{Em} < 280 \text{ nm}$  (Xiao et al., 2018c).

Fluorescence peak intensities also indicate the microbial activity of specific substances. For example, the peak intensity of coenzyme  $\text{F}_{420}$  was reported as an indicator of methanogenic activity. Dong et al. (2010) found that the fluorescence peak intensity of  $\text{F}_{420}$  was positively related to methanogenic activity in an upflow anaerobic sludge blanket (UASB) reactor. Such indicators may shed light on indications of methanogenic activity and other descriptors of operating state in anaerobic bioreactors such as anaerobic MBRs (AnMBRs). Moreover, the peak intensities of fluorescent components (i.e., component scores) obtained by decomposing the EEM spectrum using parallel factor analysis (PARAFAC) can be used to determine the formation potential of DBPs. A number of studies have reported that fluorescent tryptophan-like and amino-like components can be used to detect the formation potential of C-DBPs and N-DBPs in the process of drinking water disinfection (Yang et al., 2015; Ma et al., 2018). Humic-like and fulvic-like components and their ratios were also correlated with the formation potential of DBPs (Hua et al., 2010; Beggs and Summers, 2011; Yang et al., 2015; Watson et al., 2018). Hao et al. (2012) established a linear regression model using the peak intensities of humic acid and fulvic acid components to estimate the formation potential of DBPs (trihalomethane (THM) and haloacetic acid (HAA)). It is promising that these indicators can also be applied to MBR-based processes.

### 3.2.3 Indicators based on peak intensity ratios

The ratios between fluorescence peak intensities are also useful fluorescence indicators, including the fluorescence index (FI), humification index (HIX), biological source index (BIX), humification parameter (HP), redox index (RI), peak T/peak C, peak A/peak C, and peak B/peak C. The FI is the ratio of the fluorescence intensity of  $\text{Em } 450 \text{ nm}$  to that of  $\text{Em } 500 \text{ nm}$  at a common  $\text{Ex}$  of  $370 \text{ nm}$  ( $f_{450}/f_{500}$ ) (McKnight et al., 2001), or the ratio of the intensity of  $\text{Em } 470 \text{ nm}$  to  $\text{Em } 520 \text{ nm}$  at a common  $\text{Ex}$  of  $370 \text{ nm}$  ( $f_{470}/f_{520}$ ) (Cory and McKnight, 2005). The FI can be used to identify the sources of DOM, with  $f_{450}/f_{500}$  values of  $\sim 1.4$  and  $\sim 1.9$  for terrestrial and microbial/aquatic sources, respectively (McKnight et al., 2001; Cory and McKnight, 2005). The HIX was first proposed by Zsolnay et al. (1999) to characterize the maturity of DOM and is calculated as the ratio of the summed intensity over  $\text{Em} = 435\text{--}480 \text{ nm}$  to that over  $\text{Em} = 300\text{--}345 \text{ nm}$  at a common  $\text{Ex}$  of  $254 \text{ nm}$ . The HIX indicates the degree of humification, with a high HIX (10–16) suggesting a terrestrial origin of DOM, and a

low HIX ( $< 4$ ) suggesting in situ formation of DOM due to biological activities (Huguet et al., 2009). The BIX is defined as the ratio of the intensity of  $\text{Em } 380 \text{ nm}$  to  $\text{Em } 430 \text{ nm}$  at a common  $\text{Ex}$  of  $310 \text{ nm}$ , reflecting a recent autochthonous contribution to DOM formation (Huguet et al., 2009). The BIX values of 0.6–0.7, 0.7–0.8, and 0.8–1.0 indicate weak, intermediate, and strong autochthonous component of DOM, respectively;  $\text{BIX} > 1.0$  indicates a biological or aquatic bacterial origin of DOM (Huguet et al., 2009). He et al. (2013) proposed the HP to evaluate the degree of humification, defining it as the ratio between the sum of the integral volumes of regions III and V (fulvic acid-like and humic acid-like regions) and the sum of the integral volumes of regions I, II, and IV (protein-like regions). The HP reveals the heterogeneity of DOM, and reflects humification information more comprehensively than HIX because it is based on all the fluorescence information across the whole wavelength range. The RI is defined as the ratio of the sum of the loadings of the four reduced quinone-like components to the sum of the loadings of all seven quinone-like components identified by PARAFAC (Cory and McKnight, 2005; Miller et al., 2006), thus indicating the redox characteristic of quinone-like components of EEM. Because tryptophan-like and tyrosine-like substances are readily biodegradable whereas humic-like substances are relatively persistent, the peak T/peak C, peak A/peak C, and peak B/peak C intensity ratios can fingerprint the biodegradability of the DOM (Sheng and Yu, 2006; Liu et al., 2011; Gabor et al., 2014). The intensity integral ratio between peak C and peak T ( $I_C:I_T$ ) can be used to track dynamic changes in the fluorescent components (Zhou et al., 2017). Moreover, the ratio of the humic-like component score to the fulvic-like component score exhibited a significantly positive correlation with the potential of trihalomethane (THM) formation (Lee et al., 2018).

### 3.3 Information based on EEM deconvolution

Principal component analysis (PCA), parallel factor analysis (PARAFAC), and parallel factor framework clustering analysis (PFFCA) have been used to decompose EEM spectra. The principles and applications of these methods are described in this section.

#### 3.3.1 Principal component analysis (PCA)

PCA is a commonly used multivariate data analysis method for data compression and information extraction from a large number of variables. A set of variables that may be related to each other are transformed into a set of new independent variables, referred to as principal components (PCs) (Wold et al., 1987). PCs describe the main features of the EEM data. As shown in Eq. (1), PCA decomposes the original  $X$ -matrix of the fluorescence data

into the outer product of the vectors  $t_i$  and  $p_i$  plus a residual matrix  $E$ .

$$X = \sum_{i=1}^K t_i \times p_i + E \quad (1)$$

where  $K$  is the number of samples in the data set;  $t_i$  vectors are the scores of the PCs extracted by PCA, reflecting the projection of the original variable in the new variable space;  $p_i$  vectors are loadings that contain information about how EEM variables relate to each other, indicating the relative importance of the fluorescence variables. Two to three PCs are generally adequate to represent most of the fluorescence information.

PCA of EEM spectroscopy data has been used to analyze the characteristics of DOM in water ecosystems and water treatment processes. PCA can indicate the major components in DOM samples, including humic-like, protein-like, and particulate/colloidal organic matters (Yu et al., 2018). Peiris et al. (2010a) performed PCA to analyze the foulants in an ultrafiltration process, revealing that colloidal/particulate matter mostly contributed to reversible fouling whereas humic-like and protein-like matters were largely responsible for irreversible fouling. In addition, by tracking the variation of PCs in a water treatment plant, the removal behavior of pollutants along the process can be better elaborated (Guo et al., 2018). PCA can also distinguish the noise signals, e.g., Rayleigh scattering, from the major fluorescence signals (Peiris et al., 2010a; Peiris et al., 2010b).

### 3.3.2 Parallel factor analysis (PARAFAC)

PARAFAC comprises an alternating least squares algorithm to minimize the sum of the squares of the residuals in the trilinear model to estimate the EEM spectra (Stedmon et al., 2003). The model simplifies the EEM data set into a set of trilinear terms and an array of residuals. Assuming there are  $F$  effective components, the fluorescence intensity of the  $i$ 'th sample at the  $j$ 'th emission wavelength and the  $k$ 'th excitation wavelength is modeled as a summed product of the component score ( $a$ ), emission loading ( $b$ ), and excitation loading ( $c$ ), as shown in Eq. (2).

$$X_{ijk} = \sum_{f=1}^F a_{if} b_{jf} c_{kf} + \varepsilon_{ijk} \quad (2)$$

where  $\varepsilon_{ijk}$  is the residual term. Thus  $a$ ,  $b$  and  $c$  represent the relative concentration, the emission and the excitation spectra of the component, respectively.

EEM-PARAFAC has been applied in a variety of water ecosystems and water/wastewater treatment systems, primarily for the following aspects: (a) indication of general water quality parameters using the factor components, with the statistical significance assessed by correlation analysis (Bagtho et al., 2011; Hur and Cho, 2012;

Cohen et al., 2014); (b) indication of the humification degree of DOM using the maximum fluorescence intensity values of the factor components (He et al., 2013); (c) indication of the formation potential of DBPs (Yang et al., 2015; Ma et al., 2018); (d) investigation of microbial activities (Ruscalleda et al., 2014; Lu et al., 2017); and (e) tracking the fate of DOM in water/wastewater treatment processes (Maqbool et al., 2016). PARAFAC generally decomposes the EEM spectra of DOM into three or four components. As shown in Fig. 3(a), three types of humic-like components with different properties and behaviors exist in natural environment and engineering systems, including component 1 [Ex/Em = (< 230–260)/(400–500) nm], component 2 [Ex/Em = (< 240–275)/(434–520) and (339–420)/(434–520) nm] and component 3 [Ex/Em = (< 240–260)/(374–450) and (295–380)/(374–450) nm] (Ishii and Boyer, 2012). In addition, protein-like components are vital. As shown in Fig. 3(a), the peaks of protein components are at Ex/Em = 225/300, 280/300, 225/330, and 280/330 nm. Components at Ex/Em = 235/340 (or 290/340) nm and Ex/Em = 235/475 (or 290/475) nm represent protein-like components when both peaks appear simultaneously (Li et al., 2014; Yu et al., 2018). PARAFAC effectively separates overlapping spectra of different DOM components, enabling clear elucidation of multicomponent EEM data and further quantitative analysis (Li et al., 2014; Yu et al., 2015). However, PARAFAC is not suitable to handle nontrilinear EEM data, and fails to obtain a unique solution when processing complex environmental samples (Qian et al., 2017b). PARAFAC generally treats the Rayleigh and Raman scatterings as interfering signals but these scatterings are sometimes useful reflections of the relative concentrations of particles and colloids (Murphy et al., 2013; Wells et al., 2017).

### 3.3.3 Parallel factor framework clustering analysis (PFFCA)

PARAFAC assumes that all components are linearly independent, but this assumption becomes invalid for complex environmental cases when a single DOM molecule carries more than one fluorescent component simultaneously (i.e., these components will be highly correlated). To address this issue, a recent approach, PFFCA, recombines the collinear PARAFAC components into physically meaningful component via clustering analysis. The PFFCA process consists of two major steps: (a) decomposing the EEM data within the PARAFAC framework, and (b) clustering the components into appropriate groups (Qian et al., 2017b). For the first step, as shown in Eq. (2), the data matrix is decomposed into a set of three-line terms and residual arrays using the PARAFAC model. The factor number  $F$  is determined by increasing  $F$  until the relative squared sum of the residual is

less than a predefined threshold. Then, factors with a large variation in the scores are selected to form a data set  $G$ . For the second step, clustering analysis (e.g. hierarchical clustering) is performed on  $G$ , with the final number of clusters equal to the number of principal components of  $G$  if a PCA on  $G$  is also performed. Then each cluster represents an effective fluorescent component in the samples. Compared with PARAFAC, PFFCA can process nontrilinear EEM data (via trilinear approximations), and the resultant components are more explicable and the obtained estimates are closer to the actual EEM spectra. Moreover, PFFCA can identify and separate Raman and Rayleigh scatterings so it is unnecessary to remove them prior to the analysis (Qian et al., 2017b). Qian et al. (2017a) used PFFCA to study the chemometrics of fluorescent DOM in municipal wastewater treatment processes. Guan et al. (2018) applied PFFCA to investigate the interaction between protein and humic substances during membrane fouling.

In addition, other methods are available to analyze EEM data, including the self-organizing map (SOM), multivariate curve resolution (MCR), principal filter analysis (PFA), principal components regression (PCR), partial least squares regression (PLS), PLS discriminant analysis (PLS-DA), and soft independent modeling of class analogy (SIMCA) (Murphy et al., 2014).

## 4 Application of EEM in MBR research

### 4.1 Scope of EEM indicators for DOM characterization in MBR studies

As illustrated in Fig. 4, EEM can characterize numerous physical/chemical/biological properties of DOM in the form of the influent organics, effluent organics, SMP, EPS, and membrane foulants in MBR systems. The DOM

properties include the chemical composition, hydrophobicity, MW, degree of humification, and biodegradability. EEM has the potential to identify changes in the influent that may lead to high membrane fouling events (Peiris et al., 2010b). DOM in the effluent identified by EEM represents the efficiency of membrane retention and reflects the development of membrane fouling (Wu et al., 2013). In MBR systems, SMP and EPS play important roles in membrane fouling. Therefore, it is vital to characterize the DOM in SMP, EPS, and membrane foulants to investigate the mechanism of membrane fouling and predict the fouling trend for an early alert. As shown in Fig. 3(c), DOM from different samples (SMP, EPS, internal and external foulants) differs in the distribution of the fluorescence regions indicative of biodegradability, and fouling propensity. In addition, EEM can be used to detect the chemical composition, hydrophobicity and MW of DOM along the treatment process in MBRs, including pretreatment, biological treatment, membrane filtration, and post-treatment units. Therefore, it is essential to conduct comprehensive monitoring of the DOM in MBR systems, and EEM could be a powerful tool.

In MBR systems, a variety of factors can affect DOM properties. DOM characteristics identified by EEM can be applied to investigate how these factors (such as MBR operational conditions) affect DOM properties, thus establishing the connection between EEM and operational conditions, which helps to optimize MBR systems. These operational conditions include: (a) the food-to-microorganism (F/M) ratio, (b) SRT, (c) aeration intensity, (d) addition of carriers/adsorbents/coagulants, and (e) pretreatment of the influent. Under high F/M conditions, the high DOM concentrations in the influent are very likely to adversely affect membrane fouling (Wu et al., 2013). Different SRTs result in differences in the DOM composition of SMP and membrane foulants. It was

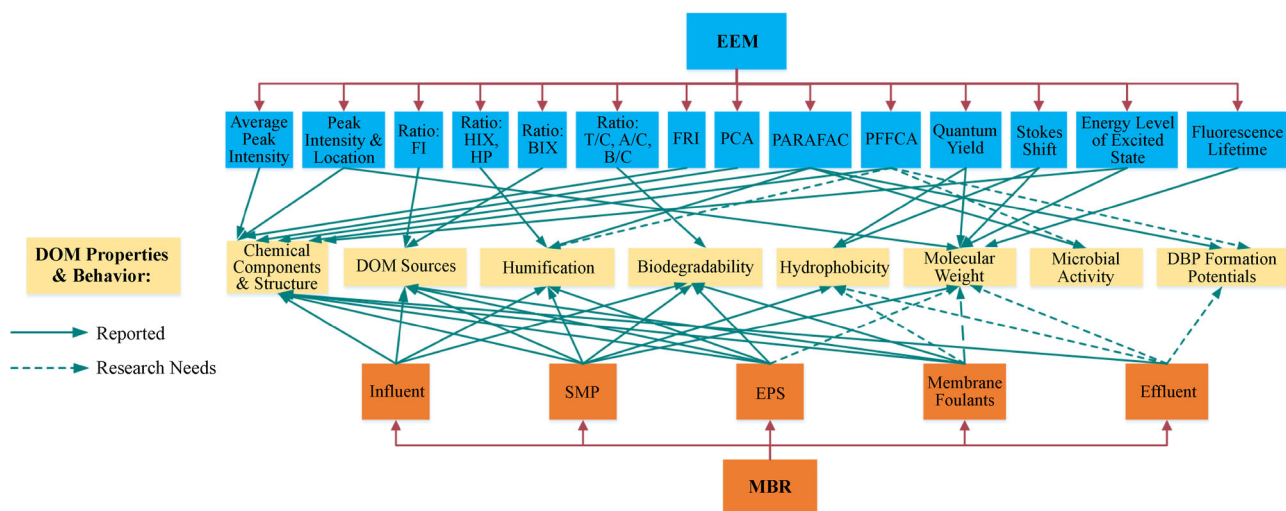


Fig. 4 Linkages between EEM properties and DOM properties for MBR studies.

reported that longer SRT resulted in a weaker fluorescence peak intensity of protein-like substances but a stronger fluorescence peak intensity of humic-like substances in SMP (Kimura et al., 2009). During the operation of an MBR, research has shown that the content of tryptophan-like components in EPS decreased with increasing aeration intensity (Maqbool et al., 2016). By adding adsorbents and carriers (such as granular activated carbon (GAC) and zeolite particles) to the MBR system, the protein-like and humic acid-like substances can be effectively removed, thereby suppressing membrane fouling (Hazrati et al., 2018). Pretreatment of the influent and mixed liquor using adsorption (Wang et al., 2017), coagulation (Deng et al., 2019), and  $O_3$  treatment (Liu et al., 2011) can also effectively control the DOM concentration and membrane fouling in MBR systems.

The linkages between EEM parameters and DOM properties/behaviors in MBR systems, including those reported previously and those meriting further study, are comprehensively summarized in Fig. 4.

#### 4.2 Characterization of pollutant transformation and degradation

EEM spectra can be used to track and monitor the transformation and degradation of pollutants in MBR systems. In terms of the spatial variation of pollutants along the process flow, EEMs in combination with FRI, PARAFAC, and other analytical methods have been effectively applied to study the fate of DOM. There are differences in the fluorescence spectra of the influent, SMP, EPS, membrane foulants, and effluent DOM. The variations in the intensity and position of each fluorescence peak and fluorescent component reflect the transfer and degradation of DOM components during the biological treatment and membrane retention process. The decrease in the intensity of fluorescence peak from the raw water to the membrane effluent generally reflects the overall degree of organic matter removal (Liu et al., 2011). The red and blue shifts of the fluorescence peaks reflect the changes in DOM structures along the process. The red shift is related to the increase of carbonyl, hydroxyl, alkoxy, and amino groups in the functional group structure (Świetlik and Sikorska, 2004) whereas the blue shift is related to the decrease in characteristic functional groups (carbonyl, hydroxyl and amine), the degree of  $\pi$ -electron conjugation, and the number of aromatic ring conjugated bonds in the carbon chain structure (Coble, 1996; Chen et al., 2002). Wang et al. (2009) reported that, in the MBR treatment process, peak A (defined in Fig. 3(a)) exhibited a red shift of 5–15 nm, peak B exhibited a red shift of 15 nm, and peak C exhibited a red shift of 10 nm in the excitation wavelength and a blue shift of 5–10 nm in the emission wavelength. Peak B represented the degradable DOM whereas peak C represented less degradable DOM. Liu et al. (2011) reported that the intensity of peaks A, T1, T2, and C

(defined in Fig. 3(a)) in the MBR influent decreased after  $O_3$  pretreatment and a red shift occurred to different degrees. From the influent to the effluent of MBR, a red shift of peaks A and T2 occurred whereas peak T1 exhibited a blue shift in the excitation wavelength. Compared with the influent and effluent, the EPS presented an increase in the intensity of peak B and a red shift of 15–35 nm for peaks A and C. Zhang et al. (2018) investigated the variations of DOM in the influent, anoxic phase, aerobic phase, and effluent of MBR by FRI analysis, demonstrating that the relative contents of tryptophan-like and tyrosine-like substances increased whereas humic-like substances decreased along the process. Other studies also confirmed the usefulness of EEM for delineating the profiles of DOM transformation, degradation, and microbial activity in MBR processes (Wang et al., 2015; Jacquin et al., 2018b).

In terms of tracking the variation of pollutants over time, EEM can record the changes in DOM characteristics during the acclimatization and operation of MBR, thus reflecting the dynamic features of pollutant degradation, microorganism activity, and operational stability. Maqbool et al. (2016 and 2017) investigated the maximum fluorescence intensity ( $F_{\max}$ ) and  $F_{\max}$  per MLSS of each EEM-PARAFAC component to track the dynamic variation in the bound EPS (bEPS), SMP, and membrane influent during the operation periods before and after acclimatization of the sludge. The  $F_{\max}$  of the tryptophan-like, tyrosine-like, and microorganism-related humic acid-like components followed the order of bEPS>SMP>effluent. To systematically compare the temporal and spatial variability of DOM properties, Xiao et al. (2018a) developed a fluorescence quotient (FQ) technique in combination with nonparametric statistical tests to evaluate the differences between any two sets of EEM fingerprints.

#### 4.3 Evaluation of the membrane retention efficacy

The retention efficiency of the membrane can be effectively evaluated by EEM. During the filtration process with fouling inevitably involved, the membrane with foulant blocking inside the pores and a gel/cake layer covering on the outer surface will serve as the de facto “membrane” as a whole. The retention efficiency of DOM could be influenced by the mechanisms of the “membrane”–DOM sieving effect, hydrophobic adsorption, and electrostatic interaction. Therefore, the retention efficiency would differ due to the differences in the MW, hydrophobicity, and electrical properties of the DOM components. EEM spectra can be used to effectively assess the ability of the “membrane” to retain different DOM components. The membrane retention rates for the tryptophan-like and tyrosine-like components were reported to be higher than that of the humic-like substances, possibly because of the higher MW (and also hydrophobicity) of the protein-like substances (Wu et al.,

2013; Jacquin et al., 2018c). In a study by Maqbool et al. (2017), the membrane retention rates of tryptophan-like, tyrosine-like, and microorganism-related humic-like substances were 99%, 99%, and 70%–80%, respectively. Yang et al. (2019) reported that the membrane retention rates of tryptophan-like and humic-like substances were 78%–90% and 40%–70%, respectively. In addition, monitoring the changes in the membrane effluent and supernatant DOM in MBR over time using EEM spectra reflects the fluctuation of membrane retention: on the one hand, enhancement of membrane retention can result from the gradual development of membrane fouling; on the other hand, a decreasing retention efficiency may reflect damage to the membrane. The retention efficiency of DOM may vary during the periods of acclimation and operation of an MBR system. In the research of Maqbool et al. (2016), the retention rates of tryptophan-like and tyrosine-like components increased after acclimation and that of the humic acid-like component decreased. Moreover, monitoring the membrane retention based on fluorescence is beneficial for early warning of membrane fouling and membrane damage (Singh et al., 2015).

#### 4.4 Exploration of membrane fouling mechanisms

Studying membrane fouling mechanisms is an important application of EEM in MBR research, and provides support to better understand fouling. The extent and reversibility of membrane fouling are closely related to the membrane–foulant and foulant–foulant interactions during fouling development. With varied physicochemical properties, the roles played by different DOM components in fouling can vary spatially (e.g., pores/interface/outer layer, from internal to external fouling) and temporally (e.g., different stages of fouling evolution, from initial adsorption/blocking to fully grown foulant layer), as illustrated in Fig. 5. These mechanisms can be profoundly elucidated by EEM analysis of the foulants.

Researchers have used EEM in combination with PARAFAC and PCA to assess the gross contribution of

different DOM components to membrane fouling in MBR. Protein-like species are well reported to have a high fouling propensity, whereas the overall contribution of humic-like species is relatively small (Wang et al., 2009; Ly and Hur, 2018). Protein-like substances are the main external membrane foulants in terms of the composition of the foulant layer (Liu et al., 2011) whereas humic-like substances dominate in internal fouling (Liu et al., 2011; Jacquin et al., 2018a). In addition, humic-like substances with different properties contribute differently to membrane fouling. Quang et al. (2016) investigated the contributions of different humic-like substances to membrane fouling using EEM-PARAFAC. They found that the protein/tannin-like components with the largest molecular weight (MW) contributed the most to membrane fouling via reversible or irreversible interaction with the membrane matrix; among the humic-like components, the subclass with the smallest MW mainly induced irreversible fouling whereas that with intermediate MW was more likely to cause reversible fouling.

In the membrane fouling stages, the membrane–foulant interaction is mainly responsible for internal fouling in the initial stage and the foulant–foulant interaction becomes predominant in external fouling during extended filtration. As schematically shown in Fig. 5, humic-like substances with relatively small particle size are adsorbed within the membrane pores due to, e.g., hydrophobic attraction, causing pore narrowing/blockage in the initial fouling stage (Wu et al., 2013; Wang et al., 2017; Jacquin et al., 2018a). With larger particle size, protein-like substances are more prone to be rejected on the membrane surface to induce concentration polarization and participate in gel/cake layer formation in long-term filtration stages (Wu et al., 2013; Wang et al., 2017; Jacquin et al., 2018a). Wang et al. (2017) found that in the initial fouling stage, the maximum fluorescence intensity ( $F_{\max}$ ) of peak A was significantly correlated with the total filtration resistance and hydraulically irreversible resistance; in long-term operation, the  $F_{\max}$  of peak T2 was significantly correlated with the total resistance, irreversible resistance, and

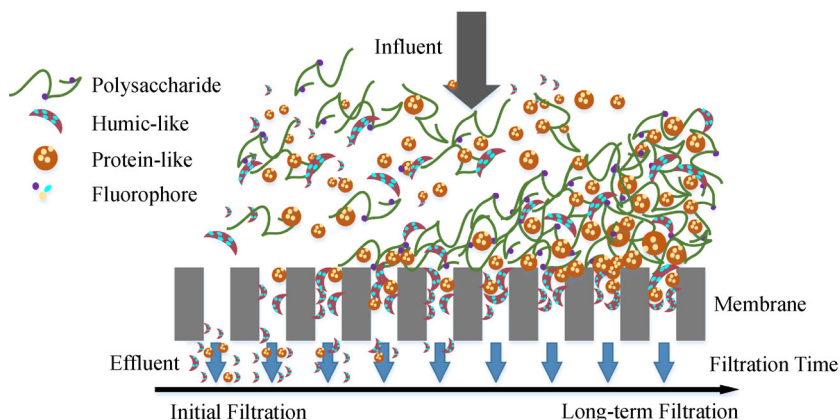


**Fig. 5** Role of DOM molecules in membrane fouling evolution at different filtration stages.

concentration polarization resistance. Guan et al. (2018) studied the effect of the electrostatic and hydrophobic interactions between coexisting humic acid and protein on membrane fouling using EEM-PFFCA. Mu et al. (2019) demonstrated that the hydrophobicity (reflected by the water contact angle) of the gel layer was strongly correlated with the overall FI/TOC ratio of the foulant EEM.

In terms of application of EEM to studying the membrane fouling mechanisms of DOM, current research is mainly focused on assessing the main DOM components causing fouling. Membrane fouling studies that combine other fluorescence indicators for DOM properties (such as hydrophobicity and MW) are still lacking. Moreover, current research is mostly limited to qualitative levels, and quantitative relationships between the fluorescence properties of DOM and membrane fouling are far from sufficient. Promisingly, there is room for further development and application of EEM in future research to understand, predict, and control membrane fouling.

#### 4.5 Evaluation of the membrane fouling control efficacy

In general, the strategies to control membrane fouling include optimization of membrane material/module/cassette, improvement of mixed liquor filterability (by adding carriers, adsorbents, coagulants, oxidants, quorum quenchers, etc.), adjustment of operating conditions (e.g., F/M, SRT and HRT for bioreactions, and flux, relaxation and aeration for the filtration), and membrane cleaning via physical/chemical/biological means (Huang et al., 2010; Wang et al., 2014; Meng et al., 2017; Xiao et al., 2019b). Early detection of the fouling potential of DOM is also important for membrane fouling control (Peiris et al., 2010b).

EEM can be used to characterize DOM in the mixed liquor, effluent, and foulant layer and, hence, evaluate variations in the foulant properties, fouling behaviors, and membrane retention performances when different measures are taken to control fouling. Liu et al. (2011) reported that pre-ozonation can reduce protein-like (peak T) signals in the EPS and external foulants, and alter the humic-like structures in the external foulants as revealed by EEM. Hazrati et al. (2018) found that zeolite nano-adsorbents can reduce protein-like and fulvic acid-like substances and mitigate fouling. However, direct relationships between the EEM spectral characteristics and fouling control performances have been rarely investigated. Straightforward EEM indicators are worth developing for early warning of the fouling tendency and convenient evaluation of the fouling control efficacy.

#### 4.6 Assessment of the impacts of online chemical cleaning

EEM spectra have also been used to study the effects of online chemical cleaning on MBR systems. Online

chemical cleaning is essential to maintain the filtration flux during long-term operation. Acidic cleaning agents (such as citric acid and HCl) are generally used for the removal of inorganic foulants deposited on the membrane, alkaline agents (such as NaOH) are used for organic foulants, and oxidant agents (such as NaClO) are used for organic and biological foulants. However, in the process of online chemical cleaning, activated sludge in the MBR system is inevitably exposed to the chemical agent. In reaction with different chemical agents, the sludge mixture will release different kinds of new DOM and cause secondary fouling (Cai et al., 2016). With the aid of EEM fingerprinting, research has shown that the DOM released from NaClO cleaning is mainly humic acid-like substances, whereas that from NaOH cleaning is mainly protein-like substances (Cai and Liu, 2018). Most of the humic-like and protein-like products due to NaClO cleaning are difficult to biodegrade and retain by the membrane. In the study of Cai et al. (2017), after chemical cleaning with 20 mg/L NaClO, 76.7% and 85.3% of the newly produced protein-like and humic-like substances were present in membrane effluent, respectively. To study the production of new DOM during chemical cleaning, employing EEM as a useful tool can help to re-evaluate the side effects of online chemical cleaning and optimize the types of chemicals and dosages used.

#### 4.7 Development of EEM online monitoring technology

With the continuous development and improvement of various EEM indicators (such as peak intensity, fluorescence indices, typical wavelength regions, and principal components), EEM can effectively indicate the DOM characteristics and water quality parameters, and be used to trace the migration and transformation of pollutants and the development of membrane fouling. EEM is expected to provide strong support for real-time monitoring, early warning, timely regulation, and intelligent management of MBR operation. Spectral technology has the potential for online monitoring of MBR systems, and several patents have been reported to employ online fluorescence monitoring systems (Gu et al., 2018). However, most of the current academic reports are limited to verifying the online monitoring capability of EEM based on offline measurement experiments, and real online monitoring has scarcely been achieved. Carstea et al. (2018) reported the first real-time monitoring of wastewater using fluorescence spectroscopy, but only used a portable fluorometer to monitor two of the fluorescence peaks, peak T and peak C, without an online EEM spectroscopy application. To the best of our knowledge, the current price of an offline laboratory fluorescence spectrophotometer is rather variable, ranging from approximately 5,000 to 40,000 USD. It is speculated that similar fluorescence devices for practical online monitoring purposes might be affordable to a range of wastewater treatment plants.

## 5 Further development of EEM for MBR studies

### 5.1 Further expansion of fluorescence indicators

The application of EEM in MBR is mostly limited to identification of changes in the peak position and intensity of fluorescent substances, leaving a large amount of other EEM fingerprinting information unexploited, such as the apparent fluorescence quantum yield, Stokes shift, excited energy state, and fluorescence lifetime. The apparent quantum yield is calculated as the ratio of the total fluorescence intensity integral to the total ultraviolet absorbance, reflecting the interference of the colored DOM (CDOM) absorbance and indicating the change in the FDOM to CDOM ratio (Wünsch et al., 2015); it is also used to indicate the hydrophobicity and MW of DOM (Xiao et al., 2016; Xiao et al., 2018c). The Stokes shift is calculated as the difference between the excitation frequency and the emission frequency, providing a large amount of information about the chemical structure of the fluorophore and its chemical environment (Lakowicz, 2006), and reflecting the MW and hydrophobicity of the DOM (Xiao et al., 2016; Xiao et al., 2019a). The average excited energy state can be reflected by the reciprocal of the root mean square of  $E_x$  and  $E_m$ , which is also related to the MW of the DOM (Xiao et al., 2016). The fluorescence lifetime can be calculated by the Strickler–Berg equation. Xiao et al. (2018c) found that when the MW of DOM is sufficiently small ( $< 0.5$  kDa) in the MBR system, the intrinsic fluorescence lifetime is significantly different from that of the overall DOM. The fluorescence lifetime reflects the molecular information of the DOM. However, applications of these valuable fluorescence characteristic parameters are still lacking in MBR studies, and research on the fluorescence characteristics of DOM in MBRs can be further expanded.

### 5.2 Dealing with the limitations of EEM

The inner-filter effect and fluorescence quenching affect the accuracy of EEM measurement, resulting in a decrease in the quantum yield and a distortion of the spectral shape. This may also interfere with the linear additivity of fluorescence peaks and the linear dependence of the fluorescence intensity upon concentration for purposes of quantitative analysis. The inner-filter effect describes the phenomenon that the fluorescence emitted from a fluorophore is partly intercepted by other light-absorbing substances that act as a filter in the path of the fluorescence toward the detector. The inner-filter effect is generally corrected by the UV–visible absorbance curve of the sample (given an absorbance  $< 1.5$  in the wavelength range considered) (Mobed et al., 1996; Kothawala et al., 2013), or diminished by diluting the sample enough (Luciani et al., 2009; Kothawala et al., 2013). Fluorescence

quenching involves alteration of the properties of the excited fluorophore due to, e.g., interaction with other molecules, which decreases the fluorescence intensity or fluorescent lifetime (Murphy et al., 2014). When measuring EEM spectra, it is essential to consider environmental factors that cause fluorescence quenching, including temperature, pH, metal ions, and oxidants (Henderson et al., 2009). To diminish the quenching effect, it is suggested that the pH be controlled in the range of 5–8 (Hudson et al., 2007), the temperature be kept constant (Hudson et al., 2007), and the samples be diluted to a sufficient extent (Henderson et al., 2009).

In principle, EEM can only detect substances with fluorescent properties, or some non-fluorescent substances physically bound with fluorescent molecules. However, because fluorescent DOM is only a part of DOM, it is difficult for EEM to cover the full range of DOM compositions. Polysaccharides in MBR systems are important substances for sludge viscosity and membrane fouling (Meng et al., 2017), and HIS contains a considerable proportion of polysaccharides with low aromaticity (Xiao et al., 2016). The fluorophore density in polysaccharides and HIS is generally low and the fluorescence signal is weak, which results in difficult fluorescence monitoring. The sugar chain structure of the polysaccharide itself does not produce fluorescence, but in the DOM complex system, the polysaccharide tends to bear certain fluorescence characteristics (such as the signals in lower Stokes shift region) due to heterozygosity or adsorption of unsaturated fragments. For MBR systems with a high polysaccharide content, to fully and accurately characterize DOM, other spectroscopy monitoring methods such as UV–visible spectroscopy can be used in combination. UV–visible spectroscopy is a useful supplement to fluorescence measurement because it can be used to correct the inner-filter effect and provide additional information on the DOM components that are less fluorescent such as polysaccharides.

In addition, because DOM is a mixture of complex organic compounds, it is difficult for EEM to be used for full quantitative analysis of DOM. As a result, EEM has been more extensively employed to qualitatively characterize DOM in MBR systems rather than quantitatively. However, in practice, with random error permitted, EEM-based semiquantitative relationships are quite achievable from a statistical perspective. Future research should further develop quantitative, or at least semiquantitative analysis of DOM using EEM.

### 5.3 Other fluorescent techniques for MBR monitoring

In addition to EEM, recently applied fluorescent techniques for monitoring in MBRs include front-face excitation-emission matrix (FF-EEM) and micro-laser induced fluorescence (micro-LIF). Unlike conventional EEM spectroscopy techniques for measuring solutions, FF-

EEM is measured by orienting the surface of a solid sample relative to an incident beam at 30°–60°, allowing for direct monitoring of fluorescent substances deposited on the membrane surface. It is beneficial to directly observe the development process of the membrane foulant layer and study the fouling mechanism (Yu et al., 2019). Micro-LIF is a visual, non-contact excitation measurement method. Concentration polarization and dynamic changes can be studied by observing the concentration distribution near the membrane surface in membrane fouling studies using Micro-LIF (Meng and Li, 2019). Extended use of these fluorescent techniques is promising for MBR studies.

## 6 Conclusions

The principles, methods, and applications of EEM for characterizing DOM in MBR systems are comprehensively summarized in this paper. To date, EEM has been successfully applied in MBR studies to indicate DOM physicochemical properties, migration and biodegradation behaviors, membrane fouling mechanisms, and the impacts of online chemical cleaning. The use of EEM for MBR online monitoring is promising. In addition to conventional EEM information with regard to the peak location/intensity and principal components, several novel fluorescent parameters are proposed for future expansion of EEM applications in MBR studies, including the apparent quantum yield, Stokes shift, excited energy state, and fluorescence lifetime. There are still limitations of EEM, and further investigations are needed to compensate for them.

**Acknowledgements** This work was supported by the National Natural Science Foundation of China (No. 51778599), the Beijing Natural Science Foundation (No. L182044), the CAS Strategic Priority Research Programmer (A) (No. XDA20050103), and the Youth Innovation Promotion Association CAS (No. 110500EA62).

## References

- Ahmad S R, Reynolds D M (1999). Monitoring of water quality using fluorescence technique: Prospect of on-line process control. *Water Research*, 33(9): 2069–2074
- Baghoth S A, Sharma S K, Amy G L (2011). Tracking natural organic matter (NOM) in a drinking water treatment plant using fluorescence excitation-emission matrices and PARAFAC. *Water Research*, 45(2): 797–809
- Bahram M, Bro R, Stedmon C, Afkhami A (2006). Handling of Rayleigh and Raman scatter for PARAFAC modeling of fluorescence data using interpolation. *Journal of Chemometrics*, 20(3–4): 99–105
- Baker A (2001). Fluorescence excitation-emission matrix characterization of some sewage-impacted rivers. *Environmental Science & Technology*, 35(5): 948–953
- Baker A (2002). Fluorescence excitation-emission matrix characterization of river waters impacted by a tissue mill effluent. *Environmental Science & Technology*, 36(7): 1377–1382
- Baker A, Curry M (2004). Fluorescence of leachates from three contrasting landfills. *Water Research*, 38(10): 2605–2613
- Baker A, Inverarity R (2004). Protein-like fluorescence intensity as a possible tool for determining river water quality. *Hydrological Processes*, 18(15): 2927–2945
- Beggs K M, Summers R S (2011). Character and chlorine reactivity of dissolved organic matter from a mountain pine beetle impacted watershed. *Environmental Science & Technology*, 45(13): 5717–5724
- Bridgeman J, Baker A, Carliell-Marquet C, Carstea E (2013). Determination of changes in wastewater quality through a treatment works using fluorescence spectroscopy. *Environmental Technology*, 34(23): 3069–3077
- Cai W, Liu J, Zhang X, Ng W J, Liu Y (2016). Generation of dissolved organic matter and byproducts from activated sludge during contact with sodium hypochlorite and its implications to on-line chemical cleaning in MBR. *Water Research*, 104: 44–52
- Cai W, Liu J, Zhu X, Zhang X, Liu Y (2017). Fate of dissolved organic matter and byproducts generated from on-line chemical cleaning with sodium hypochlorite in MBR. *Chemical Engineering Journal*, 323: 233–242
- Cai W, Liu Y (2018). Comparative study of dissolved organic matter generated from activated sludge during exposure to hypochlorite, hydrogen peroxide, acid and alkaline: Implications for on-line chemical cleaning of MBR. *Chemosphere*, 193: 295–303
- Carstea E M, Zakharova Y S, Bridgeman J (2018). Online fluorescence monitoring of effluent organic matter in wastewater treatment plants. *Journal of Environmental Engineering*, 144(5): 04018021
- Chen J, Gu B, Leboeuf E J, Pan H, Dai S (2002). Spectroscopic characterization of the structural and functional properties of natural organic matter fractions. *Chemosphere*, 48(1): 59–68
- Chen W, Westerhoff P, Leenheer J A, Booksh K (2003). Fluorescence excitation-emission matrix regional integration to quantify spectra for dissolved organic matter. *Environmental Science & Technology*, 37(24): 5701–5710
- Chen W B, Smith D S, Guéguen C (2013). Influence of water chemistry and dissolved organic matter (DOM) molecular size on copper and mercury binding determined by multiresponse fluorescence quenching. *Chemosphere*, 92(4): 351–359
- Christian E, Batista J R, Gerrity D (2017). Use of COD, TOC, and fluorescence spectroscopy to estimate BOD in wastewater. *Water Environment Research*, 89(2): 168–177
- Clark C D, Jimenez-Morais J, Jones G II, Zanardi-Lamardo E, Moore C A, Zika R G (2002). A time-resolved fluorescence study of dissolved organic matter in a riverine to marine transition zone. *Marine Chemistry*, 78(2-3): 121–135
- Coble P G (1996). Characterization of marine and terrestrial DOM in seawater using excitation-emission matrix spectroscopy. *Marine Chemistry*, 51(4): 325–346
- Cohen E, Levy G J, Borisover M (2014). Fluorescent components of organic matter in wastewater: efficacy and selectivity of the water treatment. *Water Research*, 55: 323–334
- Cory R M, McKnight D M (2005). Fluorescence spectroscopy reveals ubiquitous presence of oxidized and reduced quinones in dissolved organic matter. *Environmental Science & Technology*, 39(21): 8142–

- 8149
- Cumberland S A, Baker A (2007). The freshwater dissolved organic matter fluorescence–total organic carbon relationship. *Hydrological Processes*, 21(16): 2093–2099
- Cuss C W, Guéguen C (2015). Relationships between molecular weight and fluorescence properties for size-fractionated dissolved organic matter from fresh and aged sources. *Water Research*, 68: 487–497
- Deng L, Ngo H H, Guo W, Zhang H (2019). Pre-coagulation coupled with sponge-membrane filtration for organic matter removal and membrane fouling control during drinking water treatment. *Water Research*, 157: 155–166
- Dong F, Zhao Q B, Zhao J B, Sheng G P, Tang Y, Tong Z H, Yu H Q, Li Y Y, Harada H (2010). Monitoring the restart-up of an upflow anaerobic sludge blanket (UASB) reactor for the treatment of a soybean processing wastewater. *Bioresource Technology*, 101(6): 1722–1726
- DuBois M, Gilles K A, Hamilton J K, Rebers P A, Smith F (1956). Colorimetric method for determination of sugars and related substances. *Analytical Chemistry*, 28(3): 350–356
- Echevarría C, Valderrama C, Cortina J L, Martín I, Arnaldos M, Bernat X, De la Cal A, Boleda M R, Vega A, Teuler A, Castellví E (2019). Techno-economic evaluation and comparison of PAC-MBR and ozonation-UV revamping for organic micro-pollutants removal from urban reclaimed wastewater. *Science of the Total Environment*, 671: 288–298
- Figueiró C S M, Bastos De Oliveira D, Russo M R, Caires A R L, Rojas S S (2018). Fish farming water quality monitored by optical analysis: The potential application of UV–Vis absorption and fluorescence spectroscopy. *Aquaculture*, 490: 91–97
- Gabor R S, Baker A, Mcknight D M, Miller M P (2014). *Aquatic Organic Matter Fluorescence*. Coble, P.G., Lead, J., Baker, A., Reynolds, D.M. and Spencer, R.G.M. (eds): Cambridge Univ Press, the Pitt Building, Trumpington St., Cambridge Cb2 1rp, Cambs, Uk, 303–338
- Goletz C, Wagner M, Grübel A, Schmidt W, Korf N, Werner P (2011). Standardization of fluorescence excitation-emission-matrices in aquatic milieu. *Talanta*, 85(1): 650–656
- Gu H, Shi H, Sun Y, Lv R, Liu S, Li S (2018). Device for intelligently performing on-line detection frying oil e.g. palm oil, has emission window connected with fluorescence detector, and data processing device connected with fluorescence detector through data transmission line: UNIV CHUZHOU (UYCH-Non-standard)
- Guan Y F, Qian C, Chen W, Huang B C, Wang Y J, Yu H Q (2018). Interaction between humic acid and protein in membrane fouling process: A spectroscopic insight. *Water Research*, 145: 146–152
- Guo X, Yu H, Yan Z, Gao H, Zhang Y (2018). Tracking variations of fluorescent dissolved organic matter during wastewater treatment by accumulative fluorescence emission spectroscopy combined with principal component, second derivative and canonical correlation analyses. *Chemosphere*, 194: 463–470
- Hao R, Ren H, Li J, Ma Z, Wan H, Zheng X, Cheng S (2012). Use of three-dimensional excitation and emission matrix fluorescence spectroscopy for predicting the disinfection by-product formation potential of reclaimed water. *Water Research*, 46(17): 5765–5776
- Hazrati H, Jahanbakhshi N, Rostamizadeh M (2018). Fouling reduction in the membrane bioreactor using synthesized zeolite nano-adsorbents. *Journal of Membrane Science*, 555: 455–462
- He X S, Xi B D, Li X, Pan H W, An D, Bai S G, Li D, Cui D Y (2013). Fluorescence excitation-emission matrix spectra coupled with parallel factor and regional integration analysis to characterize organic matter humification. *Chemosphere*, 93(9): 2208–2215
- He X S, Xi B D, Wei Z M, Jiang Y H, Yang Y, An D, Cao J L, Liu H L (2011). Fluorescence excitation-emission matrix spectroscopy with regional integration analysis for characterizing composition and transformation of dissolved organic matter in landfill leachates. *Journal of Hazardous Materials*, 190(1-3): 293–299
- Henderson R K, Baker A, Murphy K R, Hambly A, Stuetz R M, Khan S J (2009). Fluorescence as a potential monitoring tool for recycled water systems: A review. *Water Research*, 43(4): 863–881
- Hua B, Veum K, Yang J, Jones J, Deng B (2010). Parallel factor analysis of fluorescence EEM spectra to identify THM precursors in lake waters. *Environmental Monitoring and Assessment*, 161(1-4): 71–81
- Huang X, Xiao K, Shen Y (2010). Recent advances in membrane bioreactor technology for wastewater treatment in China. *Frontiers of Environmental Science & Engineering in China*, 4(3): 245–271
- Huber S A, Balz A, Abert M, Pronk W (2011). Characterisation of aquatic humic and non-humic matter with size-exclusion chromatography–organic carbon detection–organic nitrogen detection (LC-OCD-OND). *Water Research*, 45(2): 879–885
- Hudson N, Baker A, Reynolds D (2007). Fluorescence analysis of dissolved organic matter in natural, waste and polluted waters: A review. *River Research and Applications*, 23(6): 631–649
- Hudson N, Baker A, Ward D, Reynolds D M, Brunson C, Carliell-Marquet C, Browning S (2008). Can fluorescence spectrometry be used as a surrogate for the Biochemical Oxygen Demand (BOD) test in water quality assessment? An example from South West England. *Science of the Total Environment*, 391(1): 149–158
- Huguet A, Vacher L, Relexans S, Saubusse S, Froidefond J M, Parlanti E (2009). Properties of fluorescent dissolved organic matter in the Gironde Estuary. *Organic Geochemistry*, 40(6): 706–719
- Hur J, Cho J (2012). Prediction of BOD, COD, and total nitrogen concentrations in a typical urban river using a fluorescence excitation-emission matrix with PARAFAC and UV absorption indices. *Sensors (Basel)*, 12(1): 972–986
- Ignatev A, Tuhkanen T (2019). Monitoring WWTP performance using size-exclusion chromatography with simultaneous UV and fluorescence detection to track recalcitrant wastewater fractions. *Chemosphere*, 214: 587–597
- Ishii S K, Boyer T H (2012). Behavior of reoccurring PARAFAC components in fluorescent dissolved organic matter in natural and engineered systems: a critical review. *Environmental Science & Technology*, 46(4): 2006–2017
- Jacquin C, Gambier N, Lesage G, Heran M (2018a). New insight into fate and fouling behavior of bulk Dissolved Organic Matter (DOM) in a full-scale membrane bioreactor for domestic wastewater treatment. *Journal of Water Process Engineering*, 22: 94–102
- Jacquin C, Lesage G, Traber J, Pronk W, Heran M (2017). Three-dimensional excitation and emission matrix fluorescence (3DEEM) for quick and pseudo-quantitative determination of protein- and humic-like substances in full-scale membrane bioreactor (MBR). *Water Research*, 118: 82–92
- Jacquin C, Monnot M, Hamza R, Kouadio Y, Zaviska F, Merle T,

- Lesage G, Héran M (2018b). Link between dissolved organic matter transformation and process performance in a membrane bioreactor for urinary nitrogen stabilization. *Environmental Science: Water Research & Technology*, 4(6): 806–819
- Jacquin C, Teychene B, Lemee L, Lesage G, Heran M (2018c). Characteristics and fouling behaviors of dissolved organic matter fractions in a full-scale submerged membrane bioreactor for municipal wastewater treatment. *Biochemical Engineering Journal*, 132: 169–181
- Jia S, Han H, Hou B, Zhuang H, Fang F, Zhao Q (2014). Treatment of coal gasification wastewater by membrane bioreactor hybrid powdered activated carbon (MBR–PAC) system. *Chemosphere*, 117: 753–759
- Kimura K, Naruse T, Watanabe Y (2009). Changes in characteristics of soluble microbial products in membrane bioreactors associated with different solid retention times: Relation to membrane fouling. *Water Research*, 43(4): 1033–1039
- Kothawala D N, Murphy K R, Stedmon C A, Weyhenmeyer G A, Tranvik L J (2013). Inner filter correction of dissolved organic matter fluorescence. *Limnology and Oceanography: Methods*, 11(12): 616–630
- Lakowicz J R (2006). *Principles of fluorescence spectroscopy*. 3rd. Baltimore: Springer
- Lawaetz A J, Stedmon C A (2009). Fluorescence intensity calibration using the Raman scatter peak of water. *Applied Spectroscopy*, 63(8): 936–940
- Lee M H, Ok Y S, Hur J (2018). Dynamic variations in dissolved organic matter and the precursors of disinfection by-products leached from biochars: Leaching experiments simulating intermittent rain events. *Environmental Pollution*, 242(Part B): 1912–1920
- Leenheer J A, Croué J P (2003). Characterizing aquatic dissolved organic matter. *Environmental Science & Technology*, 37(1): 18A–26A
- Li N, Hu Y, Lu Y Z, Zeng R J, Sheng G P (2016). In-situ biogas sparging enhances the performance of an anaerobic membrane bioreactor (AnMBR) with mesh filter in low-strength wastewater treatment. *Applied Microbiology and Biotechnology*, 100(13): 6081–6089
- Li W T, Chen S Y, Xu Z X, Li Y, Shuang C D, Li A M (2014). Characterization of dissolved organic matter in municipal wastewater using fluorescence PARAFAC analysis and chromatography multi-excitation/emission scan: A comparative study. *Environmental Science & Technology*, 48(5): 2603–2609
- Lin H J, Peng W, Zhang M J, Chen J R, Hong H C, Zhang Y (2013). A review on anaerobic membrane bioreactors: Applications, membrane fouling and future perspectives. *Desalination*, 314: 169–188
- Liu N, Xie X, Jiang H, Yang F, Yu C, Liu J (2016). Characteristics of estrogenic/antiestrogenic activities during the anoxic/aerobic biotreatment process of simulated textile dyeing wastewater. *RSC Advances*, 6(30): 25624–25632
- Liu T, Chen Z L, Yu W Z, You S J (2011). Characterization of organic membrane foulants in a submerged membrane bioreactor with pre-ozonation using three-dimensional excitation-emission matrix fluorescence spectroscopy. *Water Research*, 45(5): 2111–2121
- Lowry O H, Rosebrough N J, Farr A L, Randall R J (1951). Protein measurement with the Folin phenol reagent. *Journal of Biological Chemistry*, 193(1): 265–275
- Lu Y Z, Li N, Ding Z W, Fu L, Bai Y N, Sheng G P, Zeng R J (2017). Tracking the activity of the Anammox-DAMO process using excitation-emission matrix (EEM) fluorescence spectroscopy. *Water Research*, 122: 624–632
- Luciani X, Mounier S, Redon R, Bois A (2009). A simple correction method of inner filter effects affecting FEEM and its application to the PARAFAC decomposition. *Chemometrics and Intelligent Laboratory Systems*, 96(2): 227–238
- Ly Q V, Hur J (2018). Further insight into the roles of the chemical composition of dissolved organic matter (DOM) on ultrafiltration membranes as revealed by multiple advanced DOM characterization tools. *Chemosphere*, 201: 168–177
- Ma C, Xu H, Zhang L, Pei H, Jin Y (2018). Use of fluorescence excitation-emission matrices coupled with parallel factor analysis to monitor C- and N-DBPs formation in drinking water recovered from cyanobacteria-laden sludge dewatering. *Science of the Total Environment*, 640-641: 609–618
- Ma D, Gao Y, Gao B, Wang Y, Yue Q, Li Q (2014). Impacts of powdered activated carbon addition on trihalomethane formation reactivity of dissolved organic matter in membrane bioreactor effluent. *Chemosphere*, 117: 338–344
- Maqbool T, Cho J, Hur J (2017). Dynamic changes of dissolved organic matter in membrane bioreactors at different organic loading rates: Evidence from spectroscopic and chromatographic methods. *Bioresource Technology*, 234: 131–139
- Maqbool T, Quang V L, Cho J, Hur J (2016). Characterizing fluorescent dissolved organic matter in a membrane bioreactor via excitation-emission matrix combined with parallel factor analysis. *Bioresource Technology*, 209: 31–39
- Marhaba T F, Van D, Lippincott R L (2000). Rapid identification of dissolved organic matter fractions in water by spectral fluorescent signatures. *Water Research*, 34(14): 3543–3550
- McKnight D M, Boyer E W, Westerhoff P K, Doran P T, Kulbe T, Andersen D T (2001). Spectrofluorometric characterization of dissolved organic matter for indication of precursor organic material and aromaticity. *Limnology and Oceanography*, 46(1): 38–48
- Meng B Y, Li X Y (2019). In situ visualization of concentration polarization during membrane ultrafiltration using microscopic laser-induced fluorescence. *Environmental Science & Technology*, 53(5): 2660–2669
- Meng F, Zhang S, Oh Y, Zhou Z, Shin H S, Chae S R (2017). Fouling in membrane bioreactors: An updated review. *Water Research*, 114: 151–180
- Menniti A, Morgenroth E (2010). The influence of aeration intensity on predation and EPS production in membrane bioreactors. *Water Research*, 44(8): 2541–2553
- Miller M P, McKnight D M, Cory R M, Williams M W, Runkel R L (2006). Hyporheic exchange and fulvic acid redox reactions in an Alpine stream/wetland ecosystem, Colorado Front Range. *Environmental Science & Technology*, 40(19): 5943–5949
- Mobed J J, Hemmingsen S L, Autry J L, McGown L B (1996). Fluorescence characterization of IHSS humic substances: Total luminescence spectra with absorbance correction. *Environmental Science & Technology*, 30(10): 3061–3065
- Mu S, Wang S, Liang S, Xiao K, Fan H, Han B, Liu C, Wang X, Huang X (2019). Effect of the relative degree of foulant “hydrophobicity” on

- membrane fouling. *Journal of Membrane Science*, 570–571: 1–8
- Murphy K R, Bro R, Stedmon C A (2014). Aquatic Organic Matter Fluorescence. Baker, A., Reynolds, D.M., Lead, J., Coble, P.G. and Spencer, R.G.M. (eds). Cambridge: Cambridge University Press, 339–375
- Murphy K R, Stedmon C A, Graeber D, Bro R (2013). Fluorescence spectroscopy and multi-way techniques. *PARAFAC. Analytical Methods*, 5(23): 6557–6566
- Parlanti E, Wörz K, Geoffroy L, Lamotte M (2000). Dissolved organic matter fluorescence spectroscopy as a tool to estimate biological activity in a coastal zone submitted to anthropogenic inputs. *Organic Geochemistry*, 31(12): 1765–1781
- Peiris R H, Budman H, Moresoli C, Legge R L (2010a). Understanding fouling behaviour of ultrafiltration membrane processes and natural water using principal component analysis of fluorescence excitation-emission matrices. *Journal of Membrane Science*, 357(1–2): 62–72
- Peiris R H, Hallé C, Budman H, Moresoli C, Peldszus S, Huck P M, Legge R L (2010b). Identifying fouling events in a membrane-based drinking water treatment process using principal component analysis of fluorescence excitation-emission matrices. *Water Research*, 44(1): 185–194
- Qian C, Chen W, Li W H, Yu H Q (2017a). A chemometric analysis on the fluorescent dissolved organic matter in a full-scale sequencing batch reactor for municipal wastewater treatment. *Frontiers of Environmental Science & Engineering*, 11(4): 12
- Qian C, Wang L F, Chen W, Wang Y S, Liu X Y, Jiang H, Yu H Q (2017b). Fluorescence approach for the determination of fluorescent dissolved organic matter. *Analytical Chemistry*, 89(7): 4264–4271
- Quang V L, Kim H C, Maqbool T, Hur J (2016). Fate and fouling characteristics of fluorescent dissolved organic matter in ultrafiltration of terrestrial humic substances. *Chemosphere*, 165: 126–133
- Reynolds D M (2003). Rapid and direct determination of tryptophan in water using synchronous fluorescence spectroscopy. *Water Research*, 37(13): 3055–3060
- Reynolds D M, Ahmad S R (1997). Rapid and direct determination of wastewater BOD values using a fluorescence technique. *Water Research*, 31(8): 2012–2018
- Ruscalleda M, Sereydynska-Sobecka B, Ni B J, Arvin E, Balaguer M D, Colprim J, Smets B F (2014). Spectrometric characterization of the effluent dissolved organic matter from an anammox reactor shows correlation between the EEM signature and anammox growth. *Chemosphere*, 117: 271–277
- Sheng G P, Yu H Q (2006). Characterization of extracellular polymeric substances of aerobic and anaerobic sludge using three-dimensional excitation and emission matrix fluorescence spectroscopy. *Water Research*, 40(6): 1233–1239
- Singh S, Henderson R K, Baker A, Stuetz R M, Khan S J (2015). Online fluorescence monitoring of RO fouling and integrity: analysis of two contrasting recycled water schemes. *Environmental Science: Water Research & Technology*, 1(5): 689–698
- Stedmon C A, Markager S, Bro R (2003). Tracing dissolved organic matter in aquatic environments using a new approach to fluorescence spectroscopy. *Marine Chemistry*, 82(3–4): 239–254
- Świetlik J, Sikorska E (2004). Application of fluorescence spectroscopy in the studies of natural organic matter fractions reactivity with chlorine dioxide and ozone. *Water Research*, 38(17): 3791–3799
- Tan X, Acquah I, Liu H, Li W, Tan S (2019). A critical review on saline wastewater treatment by membrane bioreactor (MBR) from a microbial perspective. *Chemosphere*, 220: 1150–1162
- Tang S, Wang Z, Wu Z, Zhou Q (2010). Role of dissolved organic matters (DOM) in membrane fouling of membrane bioreactors for municipal wastewater treatment. *Journal of Hazardous Materials*, 178(1–3): 377–384
- Valeur B, Berberan-Santos M N (2012). *Molecular Fluorescence: Principles and Applications*. 2nd. Weinheim, Germany: Wiley-VCH
- Wang H, Ding A, Gan Z, Qu F, Cheng X, Bai L, Guo S, Li G, Liang H (2017). Fluorescent natural organic matter responsible for ultrafiltration membrane fouling: Fate, contributions and fouling mechanisms. *Chemosphere*, 182: 183–193
- Wang J, Li K, Wei Y, Cheng Y, Wei D, Li M (2015). Performance and fate of organics in a pilot MBR-NF for treating antibiotic production wastewater with recycling NF concentrate. *Chemosphere*, 121: 92–100
- Wang M, Chen Y (2018). Generation and characterization of DOM in wastewater treatment processes. *Chemosphere*, 201: 96–109
- Wang Z, Ma J, Tang C Y, Kimura K, Wang Q, Han X (2014). Membrane cleaning in membrane bioreactors: A review. *Journal of Membrane Science*, 468: 276–307
- Wang Z, Wu Z, Tang S (2009). Characterization of dissolved organic matter in a submerged membrane bioreactor by using three-dimensional excitation and emission matrix fluorescence spectroscopy. *Water Research*, 43(6): 1533–1540
- Watson K, Farré M J, Leusch F D L, Knight N (2018). Using fluorescence-parallel factor analysis for assessing disinfection by-product formation and natural organic matter removal efficiency in secondary treated synthetic drinking waters. *Science of the Total Environment*, 640–641: 31–40
- Wells M J M, Mullins G A, Bell K Y, Da Silva A K, Navarrete E M (2017). Fluorescence and quenching assessment (EEM-PARAFAC) of de facto potable reuse in the Neuse River, North Carolina, United States. *Environmental Science & Technology*, 51(23): 13592–13602
- Wold S, Esbensen K, Geladi P (1987). Principal component analysis. *Chemometrics and Intelligent Laboratory Systems*, 2(1–3): 37–52
- Wu B, Kitade T, Chong T H, Uemura T, Fane A G (2013). Impact of membrane bioreactor operating conditions on fouling behavior of reverse osmosis membranes in MBR–RO processes. *Desalination*, 311: 37–45
- Wünsch U J, Murphy K R, Stedmon C A (2015). Fluorescence quantum yields of natural organic matter and organic compounds: Implications for the fluorescence-based interpretation of organic matter composition. *Frontiers in Marine Science*, 2: 98
- Xia S, Zhou L, Zhang Z, Hermanowicz S W (2015). Removal mechanism of low-concentration Cr (VI) in a submerged membrane bioreactor activated sludge system. *Applied Microbiology and Biotechnology*, 99(12): 5351–5360
- Xiao K, Han B, Sun J, Tan J, Yu J, Liang S, Shen Y, Huang X (2019a). Stokes shift and specific fluorescence as potential indicators of organic matter hydrophobicity and molecular weight in membrane bioreactors. *Environmental Science & Technology*, 53(15): 8985–8993
- Xiao K, Liang S, Wang X, Chen C, Huang X (2019b). Current state and challenges of full-scale membrane bioreactor applications: A critical

- review. *Bioresource Technology*, 271: 473–481
- Xiao K, Liang S, Xiao A, Lei T, Tan J, Wang X, Huang X (2018a). Fluorescence quotient of excitation–emission matrices as a potential indicator of organic matter behavior in membrane bioreactors. *Environmental Science: Water Research & Technology*, 4(2): 281–290
- Xiao K, Shen Y, Liang S, Tan J, Wang X, Liang P, Huang X (2018b). Characteristic regions of the fluorescence excitation–emission matrix (EEM) to identify hydrophobic/hydrophilic contents of organic matter in membrane bioreactors. *Environmental Science & Technology*, 52(19): 11251–11258
- Xiao K, Shen Y, Sun J, Liang S, Fan H, Tan J, Wang X, Huang X, Waite T D (2018c). Correlating fluorescence spectral properties with DOM molecular weight and size distribution in wastewater treatment systems. *Environmental Science: Water Research & Technology*, 4(12): 1933–1943
- Xiao K, Shen Y X, Liang S, Liang P, Wang X M, Huang X (2014). A systematic analysis of fouling evolution and irreversibility behaviors of MBR supernatant hydrophilic/hydrophobic fractions during microfiltration. *Journal of Membrane Science*, 467: 206–216
- Xiao K, Sun J Y, Shen Y X, Liang S, Liang P, Wang X M, Huang X (2016). Fluorescence properties of dissolved organic matter as a function of hydrophobicity and molecular weight: case studies from two membrane bioreactors and an oxidation ditch. *RSC Advances*, 6(29): 24050–24059
- Yan X, Xiao K, Liang S, Lei T, Liang P, Xue T, Yu K, Guan J, Huang X (2015). Hydraulic optimization of membrane bioreactor via baffle modification using computational fluid dynamics. *Bioresource Technology*, 175: 633–637
- Yang L, Kim D, Uzun H, Karanfil T, Hur J (2015). Assessing trihalomethanes (THMs) and N-nitrosodimethylamine (NDMA) formation potentials in drinking water treatment plants using fluorescence spectroscopy and parallel factor analysis. *Chemosphere*, 121: 84–91
- Yang X, Meng L, Meng F (2019). Combination of self-organizing map and parallel factor analysis to characterize the evolution of fluorescent dissolved organic matter in a full-scale landfill leachate treatment plant. *Science of the Total Environment*, 654: 1187–1195
- Yu H, Qu F, Sun L, Liang H, Han Z, Chang H, Shao S, Li G (2015). Relationship between soluble microbial products (SMP) and effluent organic matter (EfOM): Characterized by fluorescence excitation emission matrix coupled with parallel factor analysis. *Chemosphere*, 121: 101–109
- Yu H, Wu Z, Zhang X, Qu F, Wang P, Liang H (2019). Characterization of fluorescence foulants on ultrafiltration membrane using front-face excitation–emission matrix (FF-EEM) spectroscopy: Fouling evolution and mechanism analysis. *Water Research*, 148: 546–555
- Yu M D, He X S, Xi B D, Gao R T, Zhao X W, Zhang H, Huang C H, Tan W (2018). Investigating the composition characteristics of dissolved and particulate/colloidal organic matter in effluent-dominated stream using fluorescence spectroscopy combined with multivariable analysis. *Environmental Science and Pollution Research International*, 25(9): 9132–9144
- Zhang D, Trzcinski A P, Luo J, Stuckey D C, Tan S K (2018). Fate and behavior of dissolved organic matter in a submerged anoxic-aerobic membrane bioreactor (MBR). *Environmental Science and Pollution Research International*, 25(5): 4289–4302
- Zhou Y, Shi K, Zhang Y, Jeppesen E, Liu X, Zhou Q, Wu H, Tang X, Zhu G (2017). Fluorescence peak integration ratio  $I_C:I_T$  as a new potential indicator tracing the compositional changes in chromophoric dissolved organic matter. *Science of the Total Environment*, 574: 1588–1598
- Zhuo M, Abass O K, Zhang K (2018). New insights into the treatment of real N,N-dimethylacetamide contaminated wastewater using a membrane bioreactor and its membrane fouling implications. *RSC Advances*, 8(23): 12799–12807
- Zsolnay A, Baigar E, Jimenez M, Steinweg B, Saccomandi F (1999). Differentiating with fluorescence spectroscopy the sources of dissolved organic matter in soils subjected to drying. *Chemosphere*, 38(1): 45–50